

Minimizing Task Space Fréchet Error via Efficient Incremental Graph Search

Rachel Holladay¹, Oren Salzman² and Siddhartha Srinivasa³

Abstract—We present an algorithm that generates a collision-free configuration-space path that closely follows, according to the discrete Fréchet metric, a desired path in task space. By leveraging the Fréchet metric and other tools from computational geometry, we approximate the search space using a cross-product graph. This structure allows us to efficiently search for the solution using a simple variant of Dijkstra’s graph search algorithm. Additionally, we can incrementally update and improve the solution in an anytime fashion. We compare multiple proposed densification strategies and show that our algorithm outperforms a previously proposed optimization-based approach.

I. INTRODUCTION

Our goal is to enable robots to complete complex tasks, like clearing off the dinner table or pouring glasses of water. Many of these tasks have task-specific constraints, like not tipping over plates or glasses. To successfully accomplish these tasks, robots need motion planners that respect these constraints as well as joint limits and collision constraints.

We focus on a particular type of constraint: following a reference path in task space. While we formally define this later, we can informally define it as constraining a robot’s hand (or end effector) to trace out a path.

If the reference path was provided as the result of someone physically demonstrating the desired path to the robot, a naïve solution would be to replay the recorded demonstration. However, this would prevent us from generalizing the motion and would fail in the presence of new clutter.

Furthermore, in many applications such as arc welding [1] or letter writing [2], we are only given the desired path of the end effector, not the full pose of the robot. Therefore, throughout this paper we will only assume we have access to the poses of the end effector in task space and will plan in the robot’s configuration space to generate collision-free paths in any environment.

The extra degrees of freedom in redundant manipulators allow us to plan paths that satisfy additional end effector constraints. Berenson et al. present a configuration-space planner that handles multiple constraints, including those in task space [3]. Yao and

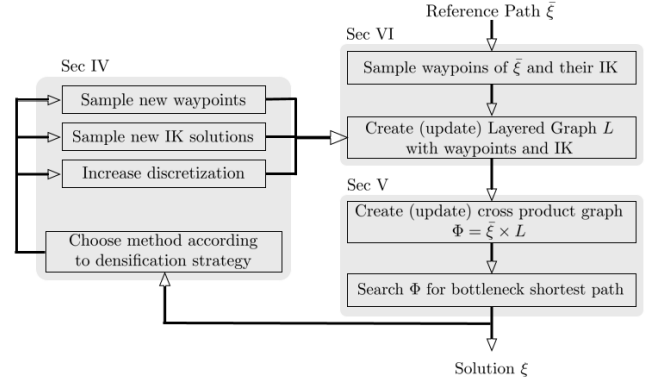


Fig. 1: A flowchart of our algorithm. We create structures that allow us to efficiently compute a path that minimizes the Fréchet distance to the reference path and incrementally densify. Each grey box outlines a major step: (1) generating candidate paths, (2) searching over paths and (3) densifying.

Gupta address the "path planning problem with general end-effector constraints (PPGEC)" by randomized gradient descent and by a search that alternates between task and configuration space, using local trajectory tracking to enforce the constraint [4]. These local trajectory tracking methods are similar to methods that focus on projecting the null space of the generalized inverse [5]. Oriolo et al. detail the limitations with these kinematic control methods [6].

Several strategies have approached this problem by optimizing or searching with respect to a particular metric. Der Einreichung used trajectory optimization with the Kullback-Leibler metric to minimize the distance between the trajectory and a distribution of reference trajectories [2]. The ROS industrial package Descartes generates candidate paths via sampling and then searches for the path that minimizes movement cost [7].

However, these methods do not optimize according to a metric that enforces the goal of the task: to follow a path. In this paper we present the Fréchet distance metric, widely used in computational geometry, as a natural way to measure the distance between paths in task space [8]. Our key insight is that using Fréchet metric to measure error allows us to efficiently organize our search for a path that closely follows our desired task-space path.

The Fréchet metric was proposed as a method for measuring distance between task-space paths in [9], which used trajectory optimization to produce a path that closely follows the reference path. However, as

¹Rachel Holladay is with the Computer Science and Artificial Intelligence Laboratory, Massachusetts Institute of Technology, rhollada@mit.edu. ²Oren Salzman is with the Robotics Institute, Carnegie Mellon University, osalzman@andrew.cmu.edu. ³Siddhartha Srinivasa is with the Paul G. Allen School of Computer Science & Engineering, University of Washington, siddh@cs.uw.edu

described in Sec. II-D, their approach suffers from the fact that it maps each task space point to one arbitrary configuration space point in the set of inverse kinematic (IK) solutions.

Instead, we search over the space of IK solutions, parameterizing the search space by task space location along the path and each point's corresponding set of IK solutions. We approximate this search space and space of the reference path as a set of simplicial complexes, which allows us to draw upon computational geometry literature to continuously approximate the discrete Fréchet distance between simplicial complexes [10]. We represent our set of simplicial complexes via one structure, which we can then efficiently search using a simple variant of Dijkstra's graph search.

This structure also allows us to densify our search, improving our solution in an anytime fashion. We describe several densification strategies that trade off between globally sampling areas and locally concentrating effort based on the results of the previous iterations. Our results show that we can more efficiently improve our solution by using the Fréchet metric to bias our search.

Fig. 1 summarizes our algorithmic approach. We first generate a set of candidate paths by sampling waypoints and their IK solutions to create a layered graph (Sec. IV). We then create a cross product graph that allows us to find a solution by searching for the bottleneck shortest path (Sec. V). By using various densification strategies, we sample and discretize to produce new candidate paths. We can efficiently incorporate these new paths by updating our structures and searching again (Sec. VI).

II. PROBLEM DEFINITION AND ALGORITHMIC BACKGROUND

We first provide definitions of configuration space, task space and their operators that will be used throughout this paper. Given these definitions we present our problem statement and describe our distance metrics.

Having specified our problem, we briefly describe the solution proposed in [9]. We explain a key shortcoming, which motivates our approach.

A. Definitions

A configuration q of our robot completely describes the location of the robot. The configuration space \mathbb{C} is the set of all configurations [11]. A path in configuration space is denoted by $\xi : [0, 1] \rightarrow \mathbb{C}$. Task space is the space defined by the pose of the robot's end effector, $SE(3)$. A path in task space is denoted as $\xi : [0, 1] \rightarrow SE(3)$.

The robot induces a forward kinematics and an inverse kinematics mapping. Forward kinematics maps configurations to task space poses, $x = FK(q)$. Inverse kinematics maps a pose in task space to a set

of robot configurations, $Q = IK(x)$ such that $Q = \{q^1, q^2, \dots, q^k\}$. In an abuse of notation we will use $FK(\xi)$ to map a configuration space path into task space path. Equipped with these definitions, we can formally define our problem.

B. Problem Statement

We are given a robot and a reference path in task space, $\bar{\xi}$ that is a polyline given by a sequence of waypoints $\{r_1 \dots r_n\} \subseteq R$ for $r_j \subseteq SE(3)$. As we will see shortly, it will be convenient to treat $\bar{\xi}$ as a (one-dimensional) graph $G_{\bar{\xi}} = (V_{\bar{\xi}}, E_{\bar{\xi}})$ where $V_{\bar{\xi}}$ are the waypoints and an edge $e \in E_{\bar{\xi}}$ connects subsequent waypoints.

Our objective is to create a collision-free path $\xi \in \mathbb{C}$ whose forward kinematics maps to a path in task space, $FK(\xi)$, that follows $\bar{\xi}$ as close as possible, where "follows" is defined formally later. Similarly to $\bar{\xi}$, our produced path ξ is a polyline represented by a sequence of waypoints. We are given a discriminative black-box collision detector that, given a point in configuration space, returns whether or not the robot would be in collision.

C. Distance Metrics

To define what it means to "follow" a path, we need a metric over task-space paths that measures how close they are. We borrow the Fréchet metric from the computational geometry literature to compare the distance between two paths in task space. A complete discussion motivating the use of the Fréchet distance as the correct metric for paths in task space can be found in [9].

Briefly, the Fréchet distance can be explained via analogy, where a dog is walking along ξ at speed parameterization α and its owner is walking along ξ at speed parameterization β . The two are connected via a leash. The Fréchet distance is the shortest possible leash via some distance metric d_{TS} such that there exists a parameterization α and β so that the two stay connected and move monotonically. More formally the continuous Fréchet distance between ξ_0 and ξ_1 is given by:

$$F(\xi_0, \xi_1) = \inf_{\alpha, \beta} \max_{t \in [0, 1]} \left\{ d_{TS}(\xi_0(\alpha(t)), \xi_1(\beta(t))) \right\}. \quad (1)$$

As is common in motion planning, we define the distance between two points, $x, y \in SE(3)$, $d_{TS}(x, y)$, as the Cartesian product of the Euclidean metric for \mathbb{R}^3 and the standard great circle solid angle metric for $SO(3)$ [12].

In practice, computing the continuous Fréchet distance is difficult and our path representation is given as a series of waypoints. Therefore, we use the discrete Fréchet distance F_d which is typically calculated via dynamic programming [13]. Adapting our metaphor to the discrete case, we replace the dog and owner with

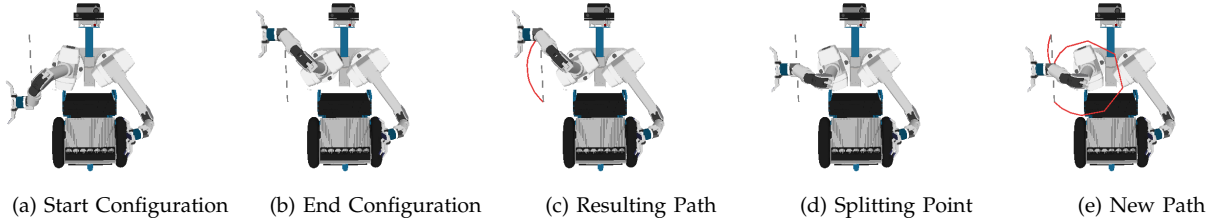


Fig. 2: The planner in [9] selects a starting and ending configuration that cannot generate a straight line path. The planner splits the path in half, only to suffer from the same problem.

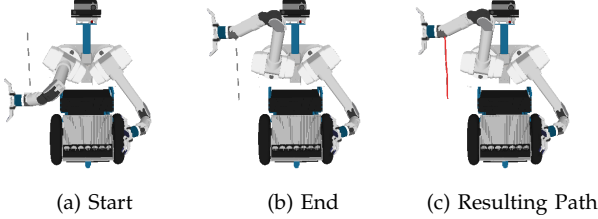


Fig. 3: The planner in [9] generate a path that matches the reference path, shown as the dotted line, because it happens to pick a starting and ending configuration that allow for a straight line path.

a pair of frogs, still attached by a leash, that can only hop along stones (our waypoints) [14].

D. Trajectory Optimization Approach

The key insight of [9] is to approximate $\bar{\xi}$ by optimizing ξ to minimize $F_d(\bar{\xi}, FK(\xi))$. Framed as a trajectory optimization problem, the paper also provides methods for assisting the optimizer by constraining the path into smaller, subdivided problems.

We examine the algorithm’s behavior on HERB, bi-manual mobile manipulator with seven degree of freedom arms (Fig. 3), as it tries to follow the straight line reference path, shown as the dotted line. The algorithm begins by picking an initial configuration (Fig. 3a) and a final configuration (Fig. 3b).

The optimizer then plans a path from the initial configuration to the final configuration, attempting to minimize the Fréchet distance between the task space reference path and the optimized path in task space. With these configurations it can drive the cost to zero, producing the solid red line path shown in Fig. 3c.

However, since there are multiple kinematic solutions in the workspace of this arm, the algorithm could have also picked the starting and ending configuration shown in Fig. 2a and Fig. 2b respectively. Given this different ending configuration, there is no path that exactly follows the reference path. Therefore the optimizer produces the red path in Fig. 2c, which significantly deviates from the reference path.

The algorithm from [9] will then split the problem at the point where the generated path deviates the most from the reference path, according to the Fréchet distance. Therefore, it splits the path in the middle and samples an IK solution, shown in Fig. 2d. As shown in Fig. 2e, the second half of the path better follows the reference path, but the first half of the path suffers from the original problem.

This limitation stems from the fact that we sample one possible IK solution for each of our start and end configurations. However, there is a space of multiple IK solutions which may admit different paths. This motivates our method, which searches over a space of IK solutions.

III. ALGORITHMIC INTUITION

Before diving into the details of our approach, we first provide an overview of our algorithmic thinking. Our goal is to find a path $\xi \in \mathbb{C}$ that minimizes $F_d(\bar{\xi}, FK(\xi))$. As mentioned in Sec. II-C, we can view the Fréchet distance as the shortest possible leash connecting the two frogs hopping along two paths, as seen at the bottom of Fig. 4a.

The red frog moves along the reference path, $\bar{\xi}$. We need to find a parameterization for the blue frog, moving along ξ , that minimizes the leash connecting the two frogs. Solving this problem is akin to searching a 2D space (shown in the top of Fig. 4a) since at each point we have the position of the two frogs.

To find the path of the blue frog, we need to search the space of IK solutions along our reference path. We can represent this by imagining that the blue frog is being carried by a redundant robot arm. Fig. 4b shows a reference path as a dotted line with three waypoints, or three positions for the blue frog. At each position, we show multiple IK solutions for the robot arm carrying the frog. Therefore we can parameterize this space, as shown in the top of Fig. 4b by the position of the blue frog along the path and the pose of the robot in that position. In Sec. IV we detail how we represent this space as a layered graph, L .

When we combine these spaces, we see that to find a path ξ with the minimum Fréchet distance to our reference path $\bar{\xi}$, we are searching along three spaces: the space defining the position of the red frog, the space defining the position of the blue frog and the space defining the pose of the robot holding the blue frog.¹ We approximate this space using one structure, the cross product graph Φ , (visualized in Fig. 4c, detailed in Sec. V).

Using results from [10], we can efficiently search this structure to find ξ that minimizes $F_d(\bar{\xi}, FK(\xi))$.

¹The dimension of the IK set is based on the number of redundant degrees of freedom. Since our task space is 6 dimensional, for N degrees of freedom, the IK set is $(N-6)D$.

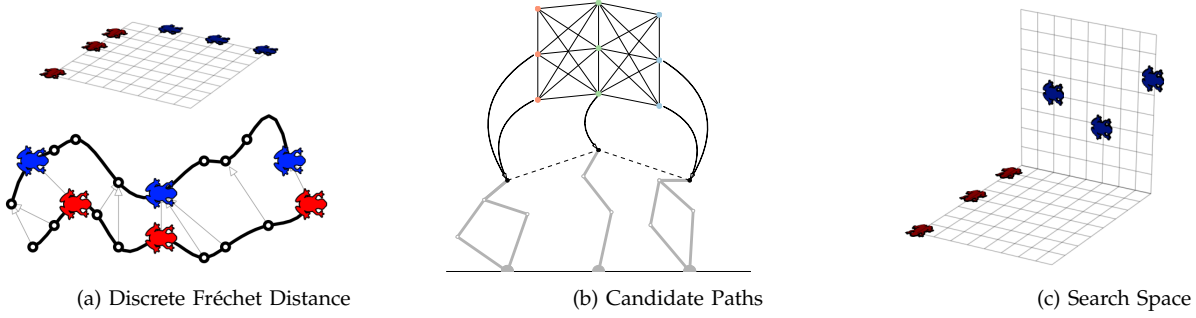


Fig. 4: Our Fréchet metric is a 2D search with respect to the position of the red and blue frogs (left). The set of candidate paths can be parameterized by the position of the blue frog and the kinematic solution of the robot holding the frog (center). Therefore searching for a candidate path with the minimum Fréchet value to our reference path can be represented by 3 parameters: position of the red frog, position of the blue frog and the set of IK solutions for each position of the blue frog (right).

While the Fréchet metric depends on the entire path, by formulating this cross-product structure, we can search across multiple candidate paths using a variant of Dijkstra’s algorithm, evaluating progress incrementally. We can also incrementally add new candidate paths via densification (Sec. VI).

IV. GENERATING A SET OF CANDIDATE PATHS

As outlined in Fig. 1, our first step is to discretely approximate the continuous space of possible paths. Following from our frog and robot example, we show that we can use two parameters to organize the space of paths into a layered graph L .

A. Layered Graph

We can restate our goal from Sec. II-B as finding a collision free path ξ such that $\min_{\xi \in \Xi} F_d(\bar{\xi}, \xi)$ where Ξ is the set of all task-space paths whose begin and end task-space poses are the same as $\bar{\xi}$. We first sample $\bar{\xi}$ for candidate paths.

Consider the set of all configuration-space paths that *exactly* map to our reference path $\bar{\xi}$. The set of all configurations along the path is:

$$S = \{q \in \mathbb{C} \mid FK(q) \in \bar{\xi}\}. \quad (2)$$

In other words, S is the set of all configurations that map to a point in task space on our reference path.

Alternatively we can define S as the inverse kinematics of all points along our reference path. Hence:

$$S = \bigcup_{\alpha \in [0,1]} IK(\bar{\xi}(\alpha)). \quad (3)$$

Thus we can use two parameters to organize our search: α , the location of a point in task space along $\bar{\xi}$, and k , an IK solutions of this point.² Hence, the limitation of [9] is that for each location α , it only considered one arbitrary configuration space solution, rather than the entire set of IK solutions. Returning to our metaphor, α corresponds to the position of the

blue frog while k corresponds to the possible inverse kinematic solutions of the robot holding the frog.

We sample this space to create a graph $L = (V_L, E_L)$ that will allow us to search for a path in configuration space. To leverage the two parameters, we construct a layered graph $L = (V_L, E_L)$ embedded in configuration space where each layer is a set of IK solutions for a waypoint (Fig. 4b).

To construct our graph, we begin by sampling n waypoints in task space along our reference trajectory: $\{r_1 \dots r_n\} \subseteq R$. At each waypoint r_j , we generate up to k IK solutions: $\{q_j^1 \dots q_j^k\}$. Each configuration q_j^i is a vertex in our graph L . Namely, the vertex set of our graph V_L is defined as: $V_L = \{q_j^i \mid 1 \leq j \leq n \text{ and } 1 \leq i \leq k\}$.

We next want to define our edge set, E_L . Each vertex in a layer of IK solutions connects to every vertex in the subsequent layer and to every vertex in its own layer. Intuitively this allows us to pass through every waypoint, with the freedom to select any IK solution for that waypoint. More formally, our edge set is defined as:

$$E_L = \{(q_j^{i_1}, q_{j+1}^{i_2}) \mid 1 \leq j_1 \leq n, 1 \leq j_2 \leq n\} \cup \{(q_j^{i_1}, q_j^{i_2}) \mid 1 \leq i_1 \leq n, 1 \leq i_2 \leq n\}. \quad (4)$$

Each of these edge represents a subpath of our entire path. Each subpath is a straight line segment in configuration space between the two configurations. We delay collision checking of these paths.

B. Naïve Search Method

Given simply our layered graph, we could restate our objective as searching for the path, ξ_L from any vertex in the first layer, q_i , to any vertex in our last layer, q_n , such that we minimize $F_d(\bar{\xi}, FK(\xi_L))$.

One naïve option would be to enumerate all candidate paths, Ξ_c and compute $F_d(\bar{\xi}, FK(\xi_c))$ for $\xi_c \in \Xi_c$. However, there are $\Omega(n^k)$ candidate paths. In this structure, since the Fréchet is a metric over the entire path, and not path segments (i.e. the individual edges), we would need to evaluate the Fréchet distance over all candidate paths.

²In practice this space might be high dimensional due to the set of inverse kinematic solutions.

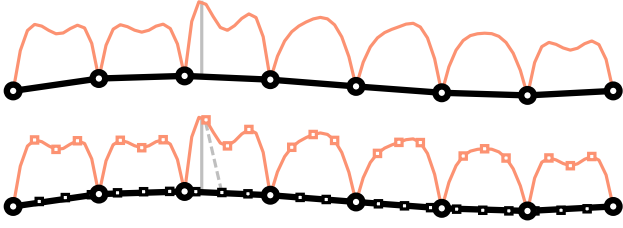


Fig. 5: We show two levels of discretization. On the top we show the reference path in black and a candidate path in task space in orange. The continuous Fréchet distance is given at the grey line but because of our discretization the discrete Fréchet distance is 0. On the bottom we show a finer level of discretization that allows us to more accurately estimate the true Fréchet distance with the discrete Fréchet distance, which is shown as the dotted grey line.

Instead we adapt a method that searches a cross product structure between our layered graph and reference path. Before doing so, we consider an example of evaluating our distance metric on the layered graph.

C. Discretization Motivation

Let's consider a layered graph L with n waypoints, for $k = 1$. Given that there is only one IK solution, this is a line graph of a single candidate path whose task space projection is $FK(\xi)$. In the top row of Fig. 5, ξ is given in black and $FK(\xi)$ in orange. The continuous Fréchet metric finds the grey line as the longest leash, with a distance of f_c . However, according to our discrete Fréchet metric $F_d(\xi, \xi_c) = 0$.

This is quite alarming—is our Fréchet distance broken? Luckily, no. Our problem stems from our choice of discretization. Our discrete Fréchet metric operates on our chosen waypoints. The vertices of our layered graph are IK solutions of the waypoints on our reference path $\bar{\xi}$. When we project these vertices back into the task space, they are at the same location of the waypoints of $\bar{\xi}$, making the distance between them zero.

In order to more accurately capture the flow of each path we need to *subsample each edge*. From Sec. IV-A, each edge is a straight line path in configuration space. We can sample configurations along this path and use inverse kinematics to generate subsampled points in configuration space. Therefore, in our layered graph we replace each edge with a path composed of these subsampled points, shown in the bottom of Fig. 5.

Here the continuous Fréchet metric finds the solid grey line as the longest leash while the discrete Fréchet metric find the longest leash as the dotted gray line. The discrete Fréchet metric is restricted to consider waypoint to waypoint distance. As we increase our discretization, our discrete Fréchet metric better approximates the continuous Fréchet distance.

Therefore, by subsampling, we increase the discretization, allowing the discrete Fréchet distance to more accurately capture the shape of the path. We can now return to the problem of creating and searching our cross product structure.

V. COMPUTING THE CLOSEST PATH

The second major step in Fig. 1 is to search over the layered graph L for a path ξ_L that minimizes $F_d(\bar{\xi}, \xi_L)$. Both our layered graph and reference path are simplicial complexes, a mathematical set composed of points, line segments, triangulations, up to n -dimensions. Har-Peled and Raichel introduced an algorithm for computing the Fréchet distance between two complexes by considering their cross product structure [10]. Therefore, our instance is a restricted case of their problem and we present our adaptation. Following Fig. 1, we first create this cross-product graph Φ and then search it for the bottleneck shortest path.

A. Cross Product Graph

We create a new graph $\Phi = (V_\Phi, E_\Phi)$ that is the cross product of our two graphs $G_{\bar{\xi}}$ and L . Each vertex in V_Φ is a tuple, (r, q) such that $r \in V_{\bar{\xi}}$ and $q \in V_L$.

We next define the edge set, E_Φ where edges exist between two tuples if either or both elements are adjacent to each other in their respective graph.

More formally:

$$E_\Phi = \{((r_{m_1}, q_{j_1}^{i_1}), (r_{m_2}, q_{j_2}^{i_2})) \mid \begin{aligned} &((q_{j_1}^{i_1}, q_{j_2}^{i_2}) \in E_L \text{ and } (r_{m_1} = r_{m_2})) \text{ or} \\ &((q_{j_1}^{i_1} = q_{j_2}^{i_2}) \text{ and } (r_{m_1}, r_{m_2}) \in E_{\bar{\xi}}) \text{ or} \\ &((q_{j_1}^{i_1}, q_{j_2}^{i_2}) \in E_L \text{ and } (r_{m_1}, r_{m_2}) \in E_{\bar{\xi}}) \}. \end{aligned} \quad (5)$$

This graph structure can be interpreted as a generalization of the typical dynamic programming for calculating the discrete Fréchet metric [13].

Given our graph Φ , we assign a cost to each edge (referred to as elevation in [10]). For a vertex (r, q) we define it's cost as $C(r, q) = d_{TS}(r, FK(q))$. The cost of an edge is then the maximum of the cost of it's endpoints.

B. Bottleneck Search

With our cross-product graph Φ , we next want to find the path with the smallest Fréchet distance. Given the construction of our graph this is equivalent to finding the path whose maximum edge cost is minimal, or the *bottleneck shortest path*. While there are efficient algorithms for this, linear in the number of edges [10], we can use a simple variant of Dijkstra's graph search [15].

Normally Dijkstra estimates the cost to vertex v coming from vertex u as the distance to u plus the cost of the edge (u, v) . However, we are interested in bottleneck, not the distance. Therefore we swap the addition, the sum of costs, for a $\max()$ such that the $\text{cost}(v) = \max(\text{cost}(u), \text{cost}(u, v))$. Therefore the bottleneck is the maximum of either the cost of the current edge or the bottleneck cost of the path leading to this edge.

While Dijkstra's algorithm, and our variant, is asymptotically larger than the linear method used in [10], $\mathcal{O}(|E| + |V| \log |V|)$, we have empirically found it to be faster and this search method allows for more

efficient updates, as described in Sec. VI. We lazily evaluate our edges for collision [16].

VI. DENSIFICATION

Sec. V considered finding the path with the smallest bottleneck cost on a fixed cross-product graph Φ . Turning to the last stage in Fig. 1, we want to consider how we can *incrementally densify* our layered graph L to improve our existing solution. Through densification, we can initialize a small layered graph and then heuristically bias our efforts on expanding the areas of the graph that may produce a path with a smaller Fréchet distance

The path from our initial fixed graph Φ has a bottleneck cost of c_0 . This cost corresponds to the most expensive edge in the path, e_i . Since the cost of the edge is determined by the maximum of the cost of the edge's endpoints, there exists some vertex $u_i \in V_\Phi$ with cost c_0 such that u_i is an endpoint of edge e_i .

To reduce the cost of our minimal bottleneck path we must find a path that avoids u_i and any vertex of equal or higher cost. As a vertex of our cross product graph Φ , u_i is a tuple (r, q) such that $r \in V_{\bar{\xi}}$ and $q \in V_L$. Remembering our definition of Fréchet distance from Sec. II-C, this means that our longest leash is between the two points (r, q) . To shorten the leash, therefore decreasing our Fréchet distance, we want to *densify our two structures*, $\bar{\xi}$ and L to provide more candidate paths to search over. By adding to $\bar{\xi}$ and L we create alternatives to u_i that hopefully create solutions that have a smaller Fréchet distance.

A. Densification Methods

To densify $\bar{\xi}$ and L we return to the parameters of their creation. Labeled as M1-M3, we can densify along the two parameters of the layered graph L or increase the discretization of either L or $\bar{\xi}$.

M1: We can densify the graph by choosing a new waypoint along our reference path and sampling k IK solutions of this waypoint. This adds an additional layer in our layered graph.

M2: We can densify the graph by sampling more inverse kinematic solutions at an existing waypoint. This increases the size of one of our existing layers.

M3: As discussed in Sec. IV-C, we discretize the edges of L and $\bar{\xi}$ to approximate the continuous Fréchet distance. We can further discretize each edge, by subsampling with higher resolution.

When we densify the layered graph L using the first two methods, we add several new vertices and edges. This, correspondingly, spawns new vertices and edges in the cross-product graph Φ .

When we increase the discretization of an edge of either L or $\bar{\xi}$, we must first remove the old subsampled edges from that structure. This is because the older edges do not approximate the continuous Fréchet distance as well as the more finely discretized edge. We then update our cross product graph accordingly.

Given our three methods of densifying our graph structures, the next question is where to apply them. For this we present several strategies, listed below.

B. Densification Strategies

Our strategies are inspired by the PRM literature, which balances between global and local updates [17], [18], [19]. Global updates sample the graph structures randomly while local updates are applied in the neighborhood of the bottleneck vertex, u_i . By sampling near the bottleneck vertex, local updates concentrate effort where the Fréchet distance is the largest.³

Below we detail how global and local updates decide where to apply each method.

Global: For M1, we randomly pick a waypoint without layer in the layered graph L and create a new layer from that waypoint. For M2, we pick a layer at random and add more IK samples. For M3, we randomly pick either the layered graph L or the reference path graph $\bar{\xi}$. From the one we select, we pick a random edge to increase the discretization.

Local: We apply our method in the neighborhood of the bottleneck vertex, $u_i = (r, q)$ for $r \in V_{\bar{\xi}}$ and $q \in V_L$. For M1, we add a layer at the layered graph at q if a layer does not already exist. For M2, we increase the size of the layer closest to q in the layered graph. For M3, we randomly choose to either the layered graph or the reference path graph. We then increase the discretization along the edge where q lies for the layered graph or where r lies for the reference path graph.

Within a single step of densification, we first determine whether to use local or global updates based on chosen strategy. We then pick a method (M1-M3) randomly. Having densified either $\bar{\xi}$ or L and updated the cross product graph Φ accordingly, we search Φ for best current solution. We formulate our search as the dynamic single-source shortest-path problem and use an efficient algorithm to reuse information from our previous searches [20], [21], [22]. This loop is illustrated in Fig. 1.

We present two strategies for balancing between global and local updates.

Hybrid: Our hybrid strategy trade offs between local and global updates by choosing local updates with probability p . We can choose purely local updates via $p = 0$ and purely global updates via $p = 1$.

Local-then-Global: This strategy combines local and global methods more intelligently across multiple steps of densification. We first focus our efforts at the bottleneck point. If this does not decrease our Fréchet distance, we switch to global updates. Since our Fréchet metric is global and considers the entire path, it is possible that, while our bottleneck occurs in one area,

³This is similar to the stapling method described in [9] in that both leverage the Fréchet metric to heuristically focus effort.

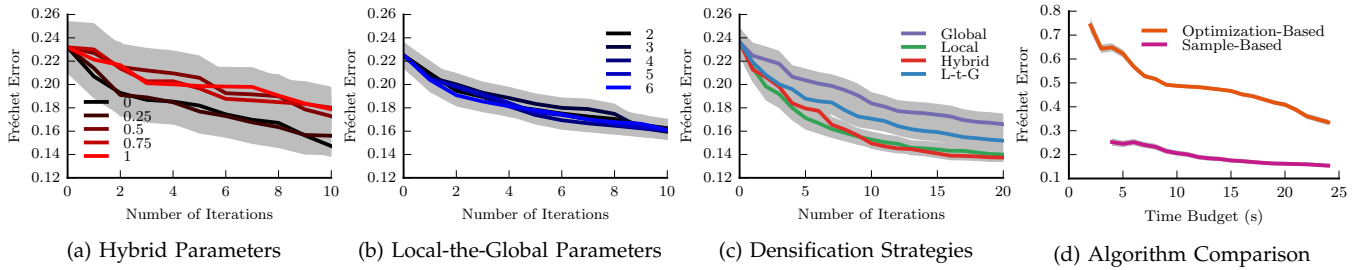


Fig. 6: The results of our parameter selection and densification strategy comparison. While each figure only show the results for one reference path and initial layered graph sizes, repeated experiments showed these results were consist across multiple reference paths and graph sizes.

the root of the problem lies somewhere else along the path.

Therefore, we first use local updates. If this succeeds, our bottleneck cost, our Fréchet distance, will decrease. While we continue to decrease our cost, we continue to use local updates. However, if m successive iterations of local updates do not decrease our cost, we switch to using global updates. If global updates reduce our cost, we return to applying local updates.

VII. EXPERIMENTAL RESULTS

We first select the parameters for both our strategies by comparing performance. We then compare all of our densification strategies against each other. Our results show that strategies that focus on local, rather than global, methods tend to excel. Finally, we compare our sample-based algorithm to the optimization approach presented in [9] and described in Sec. II-D.

Before diving into the results, we review our simulation setup. For each set of experiments we generate 100 problems with layered graphs for a given reference path $\bar{\xi}$, all with the same initial number of waypoints n , IK solutions per waypoint k , and level of edge discretization. For each problem we randomly place rectangular boxes in the environment, in the vicinity of the robot but not in collision with the reference path. We then start each densification strategy on each problem, allowing many iterations of densification.

A. Strategy Parameters

Our two strategies, hybrid and local-then-global, each have one parameter. We heuristically compare discrete choices of the parameters to select the best.

Hybrid: To explore the influence of trade off parameter p , Fig. 6a compares the path quality across $p = [0, 0.25, 0.5, 0.75, 1]$ for a fixed reference path and initial layered graph. Purely local updates correspond to $p = 0$ and purely global updates correspond to $p = 1$. We plot the Fréchet distance between the path produced at each iteration, ξ_i and the reference path, $\bar{\xi}$. We see that lower valued p 's, those that favor local updates, both produce paths with a shorter Fréchet distance at each iteration.

Local-then-Global: For our local-then-global strategy, the parameter m determines how many unsuccessful iterations of our local strategy we will iterate through before switching to a global strategy. Similarly to the

hybrid method, we compare $m = [2, 3, 4, 5, 6]$ in Fig. 6b for a fixed reference path and initial layered graph. While close, the middle value of $m = 4$ generally leads to a lower Fréchet distance at each iteration.

Therefore, in comparing our all of our densification strategies, we used $p = 0.25$ for the hybrid strategy and $m = 4$ for the local-then-global strategy.

B. Densification Strategies

Having selected the parameters for our two strategies, we now compare all four densification strategies in Fig. 6c. We compare two densification strategies along with a strategy that uses only local updates and one uses only global updates. Given the results of our parameter selection, it is unsurprising that hybrid and local strategies outperform the global strategy.

These results indicate that even while the Fréchet metric is a metric on the entire path, it is more efficient to concentrate effort in the local neighborhood of the bottleneck vertex. The hybrid and local-then-global strategies benefit from occasionally sampling global methods to avoid getting stuck densifying in one area.

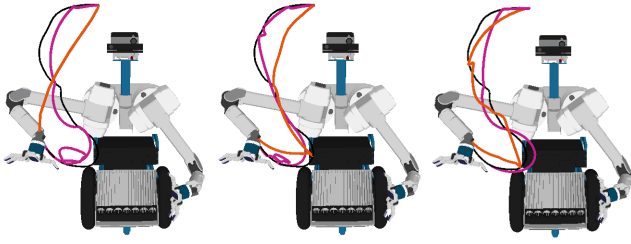
C. Search versus Optimization

Finally, we compare the sample-based approach presented in this paper to the optimization-based approach presented in [9]. The algorithm from [9], summarized in Sec. II-D, continues to split the path into subproblems until the Fréchet distance between the entire path and the reference path is below some threshold value⁴. We adapt this to an anytime algorithm where an entire trajectory is produced and evaluated after each split.

We compare the sample-based and optimization-based approaches by examining the anytime performance in Fig. 6d and their progression in Fig. 7. To compare anytime performance, we query each planner after t seconds for their best solution so far, given some time to create the initial solution.

While the optimization-based approach finds an initial solution faster, its solution is significantly worse than the one found by the sampling-based approach. As shown in Fig. 7a, the initial solution of the optimization-based approach (shown in orange) poorly

⁴In [9] this is referred to as stapling in task space.



(a) Initial Paths (b) Midway Progress (c) Final Paths

Fig. 7: We show the progression of the optimization-based approach (orange) and the sample-based approach (pink) as they try to follow the reference path (black). The obstacles in the environment are not shown for clarity.

captures the reference path (black) compared to the sample-based approach (pink). While both approaches continue to improve their solutions, with intermediate results shown in Fig. 7b, the optimization-based approach does so at a faster rate. However, given the fixed time budget, the sample-based approach produces a better quality solution (Fig. 7c).

Therefore, our sample-based approach is able to converge to a path that more closely follows the reference path because it searches over sets of IK solutions and it leverages the Fréchet metric to efficiently search.

VIII. LIMITATIONS AND FUTURE WORK

With our promising results, an immediate area of future work is providing theoretical guarantees that we would converge to the optimal solution. We also look forward to improving the efficiency of our algorithm by executing multiple iterations of densification before searching for a new solution, which would hopefully reduce time spent collision checking.

In this work we considered how to optimize paths with respect to following a given reference path. We did not consider the length of the path in the configuration space. In the future we wish to simultaneously decrease both the distance (in task space) from the reference path and the path length (in configuration space). This leads to a bicriteria optimization problem.

Finally, while we focused on generating configuration space paths for robotic manipulators to follow a task space path, the same technique can be applied to plan paths for steerable needles and concentric tube robots to allow for minimally-invasive surgery [23]. In this application, we envision the surgeon providing the reference path in task space and our algorithm producing the configuration space path for either the tip of the tube robot or the bevel edge of the steerable needle that follows the reference path.

ACKNOWLEDGMENT

This material is based upon work supported by ONR BAA 13-0001, National Science Foundation IIS (#1409003), and undergraduate research grants from CRA-W's CREU and CMU's SRC URO programs. We thank Chris Dellin for his assistance with the LPA* implementation. We would also thank the members

of the Personal Robotics Lab and the MCube Lab for helpful discussion and advice.

REFERENCES

- [1] S. Ahmad and S. Luo, "Coordinated motion control of multiple robotic devices for welding and redundancy coordination through constrained optimization in cartesian space," *TRA*, vol. 5, no. 4, pp. 409–417, 1989.
- [2] T. der Einreichung, "Combining human demonstrations and motion planning for movement primitive optimization," Master's thesis, Technische Universität Darmstadt, 2016.
- [3] D. Berenson, S. S. Srinivasa, D. Ferguson, and J. J. Kuffner, "Manipulation planning on constraint manifolds," in *ICRA*, pp. 625–632, IEEE, 2009.
- [4] Z. Yao and K. Gupta, "Path planning with general end-effector constraints," *Robotics and Autonomous Systems*, vol. 55, no. 4, pp. 316–327, 2007.
- [5] R. G. Roberts and A. A. Maciejewski, "Repeatable generalized inverse control strategies for kinematically redundant manipulators," *Transactions on Automatic Control*, vol. 38, no. 5, pp. 689–699, 1993.
- [6] G. Oriolo, M. Cefalo, and M. Vendittelli, "Repeatable motion planning for redundant robots over cyclic tasks," *Transactions on Robotics*, 2017.
- [7] ROS Industrial, "Descartes." Last updated: 3 Mar 2017.
- [8] M. M. Fréchet, "Sur quelques points du calcul fonctionnel," *Rendiconti del Circolo Matematico di Palermo (1884-1940)*, vol. 22, no. 1, pp. 1–72, 1906.
- [9] R. M. Holladay and S. S. Srinivasa, "Distance metrics and algorithms for task space path optimization," in *IROS*, pp. 5533–5540, IEEE, 2016.
- [10] S. Har-Peled and B. Raichel, "The Fréchet distance revisited and extended," *TALG*, vol. 10, no. 1, p. 3, 2014.
- [11] T. Lozano-Perez, "Spatial planning: A configuration space approach," in *Autonomous robot vehicles*, pp. 259–271, Springer, 1990.
- [12] I. A. Şucan, M. Moll, and L. E. Kavraki, "The open motion planning library," *Robotics & Automation Magazine*, vol. 19, no. 4, pp. 72–82, 2012.
- [13] T. Eiter and H. Mannila, "Computing discrete Fréchet distance," tech. rep., Citeseer, 1994.
- [14] P. K. Agarwal, R. B. Avraham, H. Kaplan, and M. Sharir, "Computing the discrete Fréchet distance in subquadratic time," *Journal on Computing*, vol. 43, no. 2, pp. 429–449, 2014.
- [15] E. W. Dijkstra, "A note on two problems in connexion with graphs," *Numerische mathematik*, vol. 1, no. 1, pp. 269–271, 1959.
- [16] C. M. Dellin and S. S. Srinivasa, "A unifying formalism for shortest path problems with expensive edge evaluations via lazy best-first search over paths with edge selectors," in *ICAPS*, pp. 459–467, 2016.
- [17] L. Kavraki and J.-C. Latombe, "Randomized preprocessing of configuration for fast path planning," in *ICRA*, pp. 2138–2145, IEEE, 1994.
- [18] L. E. Kavraki, P. Švestka, J.-C. Latombe, and M. H. Overmars, "Probabilistic roadmaps for path planning in high-dimensional configuration spaces," *TRA*, vol. 12, no. 4, pp. 566–580, 1996.
- [19] R. Bohlin and L. E. Kavraki, "Path planning using lazy PRM," in *ICRA*, vol. 1, pp. 521–528, IEEE, 2000.
- [20] D. Frigioni, A. Marchetti-Spaccamela, and U. Nanni, "Fully dynamic algorithms for maintaining shortest paths trees," *Journal of Algorithms*, vol. 34, no. 2, pp. 251–281, 2000.
- [21] G. Ramalingam and T. Reps, "On the computational complexity of dynamic graph problems," *Theoretical Computer Science*, vol. 158, no. 1, pp. 233–277, 1996.
- [22] S. Koenig, M. Likhachev, and D. Furcy, "Lifelong planning A*," *Artificial Intelligence*, vol. 155, no. 1-2, pp. 93–146, 2004.
- [23] L. G. Torres, A. Kuntz, H. B. Gilbert, P. J. Swaney, R. J. Hendrick, R. J. Webster, and R. Alterovitz, "A motion planning approach to automatic obstacle avoidance during concentric tube robot teleoperation," in *ICRA*, pp. 2361–2367, IEEE, 2015.